



Research Article

Magnetic Field Effect on Heat and Momentum of Fractional Maxwell Nanofluid within a Channel by Power Law Kernel Using Finite Difference Method

Maha M. A. Lashin,¹ Muhammad Usman,² Muhammad Imran Asjad ,³ Arfan Ali,³ Fahd Jarad ,^{4,5,6} and Taseer Muhammad⁷

¹Electrical Engineering Department, College of Engineering, Princess Nourah bint Abdulrahman University, P.O. Box 84428, Riyadh 11671, Saudi Arabia

²Department of Mathematics, National University of Modern Languages (NUML), Islamabad 44000, Pakistan

³Department of Mathematics, University of Management and Technology Lahore, Lahore, Pakistan

⁴Department of Mathematics, Cankaya University, Etimesgut, Ankara, Turkey

⁵Department of Mathematics, King Abdulaziz University, Jeddah, Saudi Arabia

⁶Department of Medical Research, China Medical University Hospital, China Medical University, Taichung, Taiwan

⁷Department of Mathematics, College of Sciences, King Khalid University, Abha 61413, Saudi Arabia

Correspondence should be addressed to Fahd Jarad; fahd@cankaya.edu.tr

Received 11 January 2022; Revised 2 March 2022; Accepted 7 March 2022; Published 23 May 2022

Academic Editor: Jawad Ahmad

Copyright © 2022 Maha M. A. Lashin et al. This is an open access article distributed under the Creative Commons Attribution License, which permits unrestricted use, distribution, and reproduction in any medium, provided the original work is properly cited.

The mathematical model of physical problems interprets physical phenomena closely. This research work is focused on numerical solution of a nonlinear mathematical model of fractional Maxwell nanofluid with the finite difference element method. Addition of nanoparticles in base fluids such as water, sodium alginate, kerosene oil, and engine oil is observed, and velocity profile and heat transfer energy profile of solutions are investigated. The finite difference method involving the discretization of time and distance parameters is applied for numerical results by using the Caputo time fractional operator. These results are plotted against different physical parameters under the effects of magnetic field. These results depicts that a slight decrease occurs for velocity for a high value of Reynolds number, while a small value of Re provides more dominant effects on velocity and temperature profile. It is observed that fractional parameters α and β show inverse behavior against $u(y, t)$ and $\theta(y, t)$. An increase in volumetric fraction of nanoparticles in base fluids decreases the temperature profile of fractional Maxwell nanofluids. Using mathematical software of MAPLE, codes are developed and executed to obtain these results.

1. Introduction

Partial differential equations (PDEs) are the best way to express physical phenomena mathematically. PDEs are widely used in many fields of engineering like bioengineering, chemical engineering, and oceanography. Few years earlier, the main focus of researchers was the integral order of these PDEs. But, for the last few decades, the fractional order of PDEs is a hot topic among scientists. This is because the fractional modeling of natural phenomena gave a new

direction to solutions of real-world problems, including diffusion, chaos, chemical reactions, dynamics, and viscoelasticity [1–3]. Approximately, all the polymeric matters have a viscoelastic behavior and conventional derivatives do not interpret such trend. Most of the fractional fluid problems are solved analytically due to the linearity of the problems. But, for the nonlinear problem, analytical techniques are complex to use. Fractional modeling of such physical problems can describe the heredity aspects and memory effect of problems. Nowadays, this idea of fractional

modeling has been published in several articles of applied mathematics, fluid dynamics, and thermal engineering. These models are formulated by using various differentiation operators such as Caputo, Caputo-Fabrizio, and Atangana–Baleanu derivatives [4, 5]. An analytical solution has been obtained via Laplace transformation, and it is concluded that fractional results are better rather than using classical derivation for temperature and velocity profile [6, 7]. These operators are used to investigate mass concentration, heat flow, and momentum along different geometries. These theories have been applied to various fluids including Cassin fluids, Brickman type fluids, Oldroyd-B fluids, and Maxwell fluids as well [8, 9]. Recently, the Maxwell models have gained much attention from researchers as it is the first and one of the simplest rate type models (RTMs). The Maxwell model is widely used to represent the response of polymeric liquids. But, this model does not express the typical relation between shear strain and shear stress [10, 11]. The research work which has already been done for fractional Maxwell fluid (FMF) modeling (particularly on analytical side) has various bounds for momentum transfer only [12–17]. An investigation has been done for FMF flow, by introducing some suitable variables to make the irregular boundary of the stretching sheet and the regular one in [18]. It can be seen [19] that Brownian motion, mass concentration, and temperature profile as well are studied for FMF flow near a moving plate by using L1-algorithm i.e., numerically. By applying Laplace and Henkel transformation jointly, flow of FMF was investigated in [20]. The recent development in modeling of FMF rather than that of simple Maxwell fluids may be seen in [21–23]. In recent days, fractional modeling of Maxwell fluids with nanomaterials is the hot issue in nanotechnology. Nanomaterials are the nanoparticles of size range from 1 nm to 100 nm. These nanosized particles are helpful to enhance the thermal conductivity of base fluids (water, sodium alginate, kerosene oil, engine oil, etc.). This idea was given for the first time by Choi and Eastman in [24], and later on, the size and shapes of different nanoparticles were investigated in a square cavity in [25]. Since the addition of nanoparticles in base fluids increases the surface area of the fluid, it consequently enhances the heat conduction of the system, i.e., control the entropy generation of heat. Analytical study has been done using Laplace transform for Caputo time derivatives of convective flow. Under the effects of magnetic field, exact solutions were obtained in [26]. Shamshuddin and Eid [27] examined heat transfer in water-based nanofluids containing ferromagnetic nanoparticles flowing between parallel stretchable spinning discs with variable viscosity influences and variable conductivities through the Chebyshev spectral collocation procedure. Unsteady flow was investigated under the effect of pressure gradient and magnetic field by using Laplace transformation as in [28]. Developing a fractional, coupled but linear PDEs model, the results were plotted against different physical parameters in [29, 30]. Similarly, it can be seen that solutions of many PDEs models are obtained analytically. After many assumptions, the models are turned into linear ones for simplicity of the problems. In [31–33], the analytical

approach is used to find the solutions of mathematical models. Also, mostly results are driven by analytical technique by many assumptions to make the model a linear one for simplicity.

The research work which has already been discussed has various research gaps in the field of nanofluids. As numerical study had not been performed, fractional behavior of mathematical models was not discussed properly with the basic tensor form. Therefore, this article deals with numerical solutions of unsteady flow of MHD-based fractional Maxwell nanofluids. This will provide the basis for further in-depth study while investigating the dynamics of FMF within a bounded channel instead of other geometric properties. Rather than the analytical technique, the strong numerical technique of the finite difference method FDM is applied to obtain solution of the FMF which involves discretization of spatial and time derivatives. The velocity profile and temperature profile have been plotted against various physical parameters by using MAPLE software. By developing and executing MAPLE coding against different physical parameters, results are obtained graphically.

2. Mathematical Modeling

The boundary layer flow within a channel is considered in this article, taking water-based nanofluids (Cu and Al_2O_3) in a vertical channel. Both the plates are separated by a distance d . One of the plates is fixed along the x -axis, vertically upward, i.e., x -axis is parallel to the plates and y -axis is normal to the plates, with B_0 strength of magnetic field. At the start, for $t = 0$, plates as well as fluids are supposed to have temperature θ_d . For some time $t > 0$, the temperature is raised to θ_0 , causing the free convection flow as illustrated in Figure 1.

Hence, the velocity field is of the form $\mathbf{V}(x, y, t) = \mathbf{V}[u(y, t), 0, 0]$. Considering the unsteady flow of water-based nanofluid in this vertical channel, the assumptions for the mathematical formulation of PDEs of the coupled and nonlinear fractional Maxwell nanofluid model is as follows:

- (i) Flow is incompressible, viscoelastic, and nonlinear
- (ii) Flow is unsteady
- (iii) Pressure gradient is neglected, i.e., $\partial P/\partial x = 0$
- (iv) A uniform magnetic field is applied along the vertical direction (along y – direction), neglecting induced magnetic field
- (v) Viscous dissipation is absent

We know that the tensor for the Maxwell fluid given in [34] is

$$\mathbf{T} = -p\mathbf{I} + \mathbf{S},$$

$$\mathbf{S} + \lambda_1 \frac{\delta \mathbf{S}}{\delta t} = \mu \mathbf{A}_1, \quad (1)$$

where \mathbf{S} , \mathbf{I} , p , \mathbf{T} , λ_1 , and \mathbf{A}_1 are the extra stress tensor, identity tensor (matrix tensor), dynamic pressure, Cauchy stress tensor, time relaxation, and first Rivlin–Ericksen tensor, respectively. And, \mathbf{DS}/\mathbf{Dt} is given in [35] and defined as

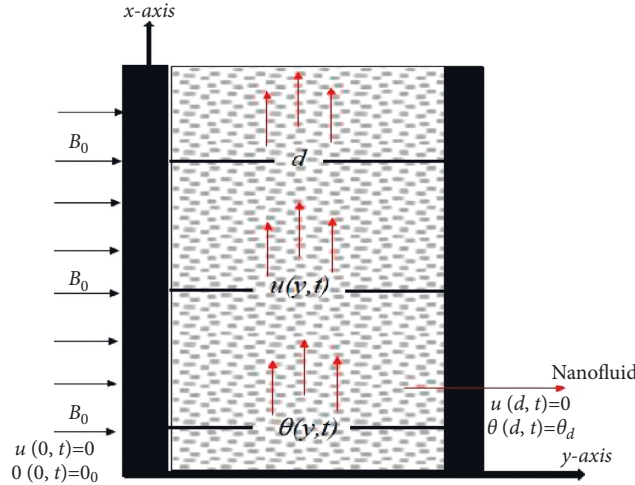


FIGURE 1: Geometry of the problem.

$$\frac{\delta \mathbf{S}}{\delta t} = \frac{D\mathbf{S}}{Dt} - \mathbf{L}\mathbf{S} - \mathbf{S}\mathbf{L}^T, \quad (2)$$

where D/Dt is the material time derivative and \mathbf{A}_1 is the first Rivlin–Ericksen tensor defined as

$$\mathbf{A}_1 = \text{grad}\mathbf{V} + (\text{grad}\mathbf{V})^T. \quad (3)$$

Using all of the above-discussed results, the constitutive relation for Maxwell fluid model is obtained [15].

$$(1 + \lambda_1^\alpha D_t^\alpha) \mathbf{S}_{xy} = \mu \frac{\partial u}{\partial y} \quad \text{with } 0 < \alpha < 1, \quad (4)$$

where \mathbf{S}_{xy} is the nonzero component of extra stress tensor, μ is the coefficient of viscosity, λ_1 is the time relaxation, and D_t^α is Caputo time fractional differentiation operator of order α , defined in [36].

$${}_0^C D_t^\alpha f(t) = \frac{1}{\Gamma(1-\alpha)} \int_0^t (t-\eta)^{-\alpha} \frac{\partial f(\eta)}{\partial \eta} d\eta, \quad 0 < \alpha < 1, \quad (5)$$

where $\Gamma(\cdot)$ is the Gamma function defined in [36].

$$\Gamma(z) = \int_0^\infty \eta^{z-1} e^{-\eta} d\eta, \quad z \in \mathbb{C}, \quad \Re(z) > 0. \quad (6)$$

Under the aforementioned assumptions, the mathematical model of this problem is as follows. The equation of continuity [37] is

$$\frac{\partial \rho}{\partial t} + \rho(\nabla \cdot \mathbf{V}) = 0, \quad (7)$$

where ρ is the density, ∇ is the gradient operator, and \mathbf{V} is a velocity field.

Here, we neglect v component of velocity along y – direction, in both momentum and energy equations. Also, taking into account the Boussinesq approximation, the momentum equation is given as in [38]

$$\rho_{nf} \frac{\partial u}{\partial t} = \frac{\partial \mathbf{S}_{xy}}{\partial y} + g(\rho\beta_\theta)_{nf}(\theta - \theta_0) - \sigma_{nf} B_0^2 u, \quad (8)$$

where ρ_{nf} is the dynamic viscosity of the nanofluid and g , $(\beta_\theta)_{nf}$, σ_{nf} , and B_0 are acceleration due to gravity, coefficient of thermal expansion of nanofluid, and coefficient of electrical conductivity for nanofluids, and magnetic field strength, respectively.

Multiplying $(1 + \lambda_1^\alpha D_t^\alpha)$ on both sides of (7),

$$(1 + \lambda_1^\alpha D_t^\alpha) \rho_{nf} \frac{\partial u}{\partial t} = (1 + \lambda_1^\alpha D_t^\alpha) \frac{\partial \mathbf{S}_{xy}}{\partial y} + g(\rho\beta_\theta)_{nf} (1 + \lambda_1^\alpha D_t^\alpha) (\theta - \theta_0) - \sigma_{nf} B_0^2 (1 + \lambda_1^\alpha D_t^\alpha) u. \quad (9)$$

Using $(1 + \lambda_1^\alpha D_t^\alpha) \mathbf{S}_{xy} = \mu_{nf} \partial u / \partial y$, the constitutive relation for Maxwell fluid in [39] is

$$(1 + \lambda_1^\alpha D_t^\alpha) \rho_{nf} \frac{\partial u}{\partial t} = \mu_{nf} \frac{\partial^2 u}{\partial y^2} + (1 + \lambda_1^\alpha D_t^\alpha) g(\rho\beta_\theta)_{nf} (\theta - \theta_0) - (1 + \lambda_1^\alpha D_t^\alpha) \sigma_{nf} B_0^2 u. \quad (10)$$

Also, the energy equation in the presence of Joule's heating effect in [38] is

$$(\rho C_p)_{nf} \left(\frac{\partial \theta}{\partial t} \right) = -\frac{\partial q}{\partial y} + \sigma_{nf} B_0^2 u^2. \quad (11)$$

$$(1 + \lambda_2^\beta D_t^\beta)(\rho C_p)_{nf} \left(\frac{\partial \theta}{\partial t} \right) = -\frac{\partial}{\partial y} (1 + \lambda_2^\beta D_t^\beta) q + \sigma_{nf} B_0^2 (1 + \lambda_2^\beta D_t^\beta) u^2. \quad (12)$$

But, by fractional Cattaneo's Law [40],

$$(1 + \lambda_2^\beta D_t^\beta) q = -k_{nf} \frac{\partial \theta}{\partial y}. \quad (13)$$

Hence, (11) becomes

$$(1 + \lambda_2^\beta D_t^\beta)(\rho C_p)_{nf} \left(\frac{\partial \theta}{\partial t} \right) = k_{nf} \frac{\partial^2 \theta}{\partial y^2} + \sigma_{nf} B_0^2 (1 + \lambda_2^\beta D_t^\beta) u^2. \quad (14)$$

It has the following initial and boundary conditions:

$$\begin{aligned} u(y, 0) &= 0, \\ u(0, t) &= 0, \\ u(d, t) &= 0, \\ \theta(y, 0) &= \theta_0, \\ \theta(0, t) &= \theta_0, \\ \theta(d, t) &= \theta_d. \end{aligned} \quad (15)$$

Employ the following transformation for the channel flow:

$$\begin{aligned} u^* &= \frac{d}{\nu_f} u, \\ x^* &= \frac{x}{d}, \\ t^* &= \frac{\nu_f}{d^2} t, \end{aligned}$$

Applying $(1 + \lambda_2^\beta D_t^\beta)$ on both sides of (10),

$$\begin{aligned} \theta^* &= \frac{\theta - \theta_0}{\theta_d - \theta_0}, \\ \lambda_1^* &= \frac{\nu_f}{d^2} \lambda_1, \\ \lambda_2^* &= \frac{\nu_f}{d^2} \lambda_2, \\ y^* &= \frac{y}{d}, \\ M^* &= \frac{\sigma_f B_0^2 \nu_f}{(\rho C_p)_f (\theta_d - \theta_0)}, \\ Ha^2 &= M = \frac{d^2 \sigma_f B_0^2}{\mu_f}, \\ Pr &= \frac{(\mu C_p)_f}{K_f}, \\ Gr &= \frac{d^3 g (\beta_\theta)_f (\theta_d - \theta_0)}{\nu_f^2}, \\ \frac{1}{Re} &= \frac{\mu}{\rho U_0 d}. \end{aligned} \quad (16)$$

Here, $Ha = M$, Pr , M^* , and Gr given in [41] are the square of Hartmann number, Prandtl number, Joule's heating parameter, and Grashof number, respectively. The following governing equations for velocity and temperature profile are obtained after omitting “*” notation for the sake of brevity of mathematical modeling:

$$(1 + \lambda_1^\alpha D_t^\alpha) \left(\frac{\partial u}{\partial t} \right) = b_1 \frac{\partial^2 u}{\partial y^2} + (1 + \lambda_1^\alpha D_t^\alpha) b_2 Gr \theta - b_3 M (1 + \lambda_1^\alpha D_t^\alpha) u, \quad (17)$$

$$(1 + \lambda_2^\beta D_t^\beta) \left(\frac{\partial \theta}{\partial t} \right) = b_4 \frac{1}{Pr} \frac{\partial^2 \theta}{\partial y^2} + b_5 M^* (1 + \lambda_2^\beta D_t^\beta) u^2. \quad (18)$$

Here, $b_1 = a_3/a_1$, $b_2 = a_2/a_1$, $b_3 = a_6/a_1$, $b_4 = a_5/a_4$, and $b_5 = a_6/a_4$. But, thermophysical properties for nanofluids in [42, 43] are known.

$$\left. \begin{aligned} \frac{\rho_{nf}}{\rho_f} = a_1 &= \left[(1 - \phi) + \phi \frac{\rho_s}{\rho_f} \right], & \frac{(\rho\beta\theta)_{nf}}{(\rho\beta\theta)_f} = a_2 &= \left[(1 - \phi) + \phi \left(\frac{(\rho\beta\theta)_s}{(\rho\beta\theta)_f} \right) \right] \\ \frac{\mu_{nf}}{\mu_f} = a_3 &= \frac{1}{(1 - \phi)^{2.5}}, & \frac{(\rho C_p)_{nf}}{(\rho C_p)_f} = a_4 &= \left[(1 - \phi) + \phi \left(\frac{(\rho C_p)_s}{(\rho C_p)_f} \right) \right] \\ \frac{k_{nf}}{k_f} = a_5 &= \frac{(k_s + 2k_f) - 2\phi(k_f - k_s)}{(k_s + 2k_f) + \phi(k_f - k_s)}, & \frac{(\sigma)_{nf}}{(\sigma)_f} = a_6 &= 1 + \frac{3(\sigma_s/\sigma_f - 1)\phi}{(\sigma_s/\sigma_f - 2) - (\sigma_s/\sigma_f - 1)\phi} \end{aligned} \right\}. \quad (19)$$

By using nondimensional parameters, the initial and boundary conditions are as follows:

$$\begin{aligned} u(y, 0) &= 0, \\ u(0, t) &= 0, \\ u(1, t) &= 0, \end{aligned} \quad (20)$$

$$\begin{aligned} \theta(y, 0) &= 0, \\ \theta(0, t) &= 0, \\ \theta(1, t) &= 1. \end{aligned} \quad (21)$$

Thus, governing equations (17) and (18) for the velocity and temperature profile of fractional Maxwell nanofluid with initial and boundary conditions represented in (20)-(21) express the physical phenomena of the coupled nonlinear model. Also, physical properties of nanoparticles presented in (17) with some thermophysical properties of base fluids and nanoparticles given in Table 1 are used for numerical results.

3. Skin Friction and Nusselt Number

For measuring shear stress and heat transfer effects in an ordinary integer order system, local skin friction and Nusselt number are defined in [44] as follows:

$$\begin{aligned} C_f &= \frac{\mu}{\rho U_0^2} \left(\frac{\partial u}{\partial y} \right)_{y=0}, \\ Nu &= \frac{-kd}{\theta_w - \theta_0} \left(\frac{\partial \theta}{\partial y} \right)_{y=0}. \end{aligned} \quad (22)$$

The skin friction coefficient and local Nusselt number for (FMF) can be written by using (3) that is the fractional stress tensor for Maxwell fluid on the plate with fractional time Caputo derivative (details can be seen in [45]).

$$C_f + \lambda_1^\alpha \frac{\partial^\alpha S_f}{\partial t^\alpha} = \frac{\mu}{\rho U_0^2} \left(\frac{\partial u}{\partial y} \right)_{y=0}, \quad (23)$$

$$Nu + \lambda_1^\beta \frac{\partial^\beta Nu}{\partial t^\beta} = \frac{kd}{\theta_d - \theta_0} \left(\frac{\partial \theta}{\partial y} \right)_{y=0}. \quad (24)$$

The nondimensional form of (23)-(24) is given as

$$C_f + \lambda_1^\alpha \frac{\partial^\alpha S_f}{\partial t^\alpha} = \frac{1}{Re^2} \left(\frac{\partial u}{\partial y} \right)_{y=0}. \quad (25)$$

$$Nu + \lambda_1^\beta \frac{\partial^\beta Nu}{\partial t^\beta} = \frac{k_{nf}}{k_f} \left(\frac{\partial \theta}{\partial y} \right)_{y=0}. \quad (26)$$

4. Numerical Procedure

The discretization of the method for fractional-order model, ${}_0^C D_t^\alpha u$, ${}_0^C D_t^{1+\alpha} u$ when $0 < \alpha \leq 1$, u_t and u_{yy} , is specified as follows:

$${}_0^C D_{t_{j+1}}^\alpha u(y_i, t_{j+1}) = \frac{\lambda_1^\alpha t^{-\alpha}}{\Gamma(2-\alpha)} [u_i^{j+1} - u_i^j] + \frac{\lambda_1^\alpha t^{-\alpha}}{\Gamma(2-\alpha)} \sum_{l=1}^j (u_i^{j-l+1} - u_i^{j-l}) d_l^\alpha, \quad (27)$$

$${}_0^C D_{t_{j+1}}^{1+\alpha} u(y_i, t_{j+1}) = \frac{\lambda_1^\alpha t^{-(1+\alpha)}}{\Gamma(2-\alpha)} [u_i^{j+1} - 2u_i^j + u_i^{j-1}] + \frac{\lambda_1^\alpha t^{-(1+\alpha)}}{\Gamma(2-\alpha)} \times \sum_{l=1}^j (u_i^{j-l+1} - 2u_i^{j-l} + u_i^{j-l-1}) d_l^\alpha, \quad (28)$$

TABLE 1: Thermophysical properties of some base fluids and nanoparticles.

Materials	ρ (kgm ⁻³)	C_p (Jkg ⁻¹ k ⁻¹)	k (Wm ⁻¹ k ⁻¹)	$\beta * 10^{-5}$ (k ⁻¹)	σ (Ω m) ⁻¹
Water	997	4197	0.613	21	0.05
Copper	8933	385	400	1.67	$5.96 * 10^7$
Alumina	3970	765	40	0.85	$2.6 * 10^6$

$$\begin{aligned} \frac{\partial}{\partial t} u(y_i, t_{j+1})|_{t=t_{j+1}} &= \frac{1}{\Delta t} [u_i^{j+1} - u_i^j], \\ \frac{\partial^2}{\partial y^2} u(y_{i+1}, t_j)|_{y=y_{i+1}} &= \frac{1}{\Delta y^2} [u_{i+1}^{j+1} - 2u_i^{j+1} + u_{i-1}^{j+1}]. \end{aligned} \quad (29)$$

The nonlinear term is approximated by means of the following concept:

$$u^2(y_i, t_j) = u(y_i, t_{j+1})u(y_i, t_j). \quad (30)$$

In (27)-(28), $d_l^\alpha = -l^{1-\alpha} + (1+l)^{1-\alpha}$ when $l = 1, 2, 3, \dots, j$. A rectilinear grid is considered for investigating the numerical solution of the deliberated fluid model through

grid spacing $\Delta t > 0$ and $\Delta y > 0$ in time and space directions separately; here, $\Delta y = L/M$ and $\Delta t = T/N$ where $\Delta y, \Delta t \in \mathbb{Z}^+$. The inner grid points (y_i, t_j) in the considered domain $\Omega = [0, T] \times [0, L]$ are defined as $i\Delta y = y_i$ and $j\Delta t = t_j$. Discretization of the discussed problem at each inner grid point is given as

$$\begin{aligned} &1/\Delta t (u_i^{j+1} - u_i^j) + \frac{\lambda_1^\alpha \Delta t^{-(1+\alpha)}}{\Gamma(2-\alpha)} (u_i^{j+1} - 2u_i^j + u_i^{j-1}) + \frac{\lambda_1^\alpha \Delta t^{-(1+\alpha)}}{\Gamma(2-\alpha)} \\ &\times \sum_{l=1}^j (u_i^{j-l+1} - 2u_i^{j-l} + u_i^{j-l-1}) b_l^\alpha = \frac{b_1}{\Delta y^2} (u_{i+1}^{j+1} - 2u_i^{j+1} + u_{i-1}^{j+1}) + b_2 Gr \theta_i^{j+1} \\ &+ \frac{b_2 Gr \Delta t^{-\alpha}}{\Gamma(2-\alpha)} (\theta_i^{j+1} - \theta_i^j) + \frac{b_2 Gr \Delta t^{-\alpha}}{\Gamma(2-\alpha)} \sum_{l=1}^j (\theta_i^{j-l+1} - \theta_i^{j-l}) b_l^\alpha \\ &- \frac{b_3 Ha^2 \Delta t^{-\alpha}}{\Gamma(2-\alpha)} (u_i^{j+1} - u_i^j) + \frac{b_3 Ha^2 \Delta t^{-\alpha}}{\Gamma(2-\alpha)} \sum_{l=1}^j (u_i^{j-l+1} - u_i^{j-l}) b_l^\alpha. \end{aligned} \quad (31)$$

Also,

$$\begin{aligned} &\frac{1}{\Delta t} (\theta_i^{j+1} - \theta_i^j) + \frac{\lambda_1^\beta \Delta t^{-(1+\beta)}}{\Gamma(2-\beta)} (\theta_i^{j+1} - 2\theta_i^j + \theta_i^{j-1}) \\ &+ \frac{\lambda_1^\beta \Delta t^{-(1+\beta)}}{\Gamma(2-\beta)} \sum_{l=1}^j (\theta_i^{j-l+1} - 2\theta_i^{j-l} + \theta_i^{j-l-1}) b_l^\beta = \frac{b_4}{Pr \Delta y^2} (\theta_{i+1}^{j+1} - 2\theta_i^{j+1} + \theta_{i-1}^{j+1}) \\ &+ b_5 M^* u_i^j \left(u_i^{j+1} + \frac{\lambda_1^\beta \Delta t^{-\beta}}{\Gamma(2-\beta)} \left(u_i^{j+1} - u_i^j - \sum_{l=1}^j (u_i^{j-l+1} - u_i^{j-l}) b_l^\alpha \right) \right), \end{aligned} \quad (32)$$

for $j = 1, 2, 3, \dots, N-1$ and $i = 1, 2, 3, \dots, N-1$.

The simplest form of the above discretization is given as

$$\begin{aligned}
& -\frac{b_1}{\Delta y^2} u_{i+1}^{j+1} + \left(\frac{1}{\Delta t} - \frac{\lambda_1^\alpha \Delta t^{-1-\alpha}}{\Gamma(2-\alpha)} + \frac{2b_1}{\Delta y^2} + \frac{b_3 Ha^2 \Delta t^{-\alpha}}{\Gamma(2-\alpha)} \right) u_i^{j+1} - \frac{b_1}{\Delta y^2} u_{i-1}^{j+1} \\
& - b_2 Gr \left(1 + \frac{\Delta t^{-\alpha}}{\Gamma(2-\alpha)} \right) \theta_i^{j+1} = \left(\frac{1}{\Delta t} + \frac{2\lambda_1^\alpha \Delta t^{-1-\alpha}}{\Gamma(2-\alpha)} + \frac{b_3 Ha^2 \Delta t^{-\alpha}}{\Gamma(2-\alpha)} \right) u_i^j - \frac{b_2 Gr \Delta t^{-\alpha}}{\Gamma(2-\alpha)} \theta_i^j \\
& - \frac{\lambda_1^\alpha \Delta t^{-1-\alpha}}{\Gamma(2-\alpha)} u_i^{j-1} = F_{i,j}, \\
& - \frac{b_4}{Pr \Delta y^2} \theta_{i+1}^{j+1} + \left(\frac{1}{\Delta t} + \frac{\lambda_1^\beta \Delta t^{-1-\beta}}{\Gamma(2-\beta)} + \frac{2b_4}{Pr \Delta y^2} \right) \theta_i^{j+1} - \frac{b_4}{Pr \Delta y^2} \theta_{i-1}^{j+1} = \left(1/\Delta t - \frac{2\lambda_1^\beta \Delta t^{-1-\beta}}{\Gamma(2-\beta)} \right) \theta_i^j \\
& - \frac{\lambda_1^\beta \Delta t^{-1-\beta}}{\Gamma(2-\beta)} \theta_i^{j-1} + G_{i,j} + N_{i,j},
\end{aligned} \tag{33}$$

with the following initial and boundary conditions

$$\begin{aligned}
u_i^0 &= 0, \\
u_i^1 &= u_i^{-1}, \\
\theta_i^0 &= 0, \\
\theta_i^1 &= \theta_i^{-1}, \quad \text{for } i = 0, 1, 2, 3, \dots, M, \\
u_0^j &= 0, \\
u_M^j &= 0, \\
\theta_0^j &= 0, \\
\theta_M^j &= 1, \quad \text{for } j = 0, 1, 2, 3, \dots, N-1,
\end{aligned} \tag{34}$$

where

$$\begin{aligned}
F_{i,j} &= -\frac{\lambda_1^\alpha \Delta t^{-(1+\alpha)}}{\Gamma(2-\alpha)} \sum_{l=1}^j (u_i^{j-l+1} - 2u_i^{j-l} + u_i^{j-l-1}) b_l^\alpha + \frac{b_2 Gr \Delta t^{-\alpha}}{\Gamma(2-\alpha)} \sum_{l=1}^j (\theta_i^{j-l+1} - \theta_i^{j-l}) b_l^\alpha + \frac{b_3 Ha^2 \Delta t^{-\alpha}}{\Gamma(2-\alpha)} \sum_{l=1}^j (u_i^{j-l+1} - u_i^{j-l}) b_l^\alpha, \\
G_{i,j} &= -\frac{\lambda_1^\beta \Delta t^{-(1+\beta)}}{\Gamma(2-\beta)} \sum_{l=1}^j (\theta_i^{j-l+1} - 2\theta_i^{j-l} + \theta_i^{j-l-1}) b_l^\beta, \\
N_{i,j} &= b_5 M^* u_i^j \left(u_i^{j+1} + \frac{\lambda_1^\beta \Delta t^{-\beta}}{\Gamma(2-\beta)} \left(u_i^{j+1} - u_i^j - \sum_{l=1}^j (u_i^{j-l+1} - u_i^{j-l}) b_l^\alpha \right) \right).
\end{aligned} \tag{35}$$

$$U(y, 0) = U(0, t) = U(d, t) = 0. \tag{37}$$

5. Numerical Analysis and Discussion

5.1. *Test Problem.* Consider the following problem:

$${}^c D_t^\alpha U(y, t) = \frac{\partial^2}{\partial y^2} U(y, t) - \frac{\partial}{\partial y} U(y, t) + h(y, t). \tag{36}$$

Here, the conditions are given as follows and source term can be selected against the choice of fractional-order derivative:

The exact solution of this problem is $U(y, t) = y(y-t)t^2$. Various simulations have been performed to check the accuracy of the proposed scheme. Figures 1(a) and 1(b) are plotted for maximum absolute error (MAE) and computational order of convergence (COC) given as follows when $N = 10, 20, 40, 80, 160, 320, 640$:

$$\begin{aligned} \text{MAE} &= \max_{\substack{1 \leq i \leq M \\ 1 \leq j \leq N}} |U(y_i, t_j) - U_i^j|, \\ \text{COC} &= \log \frac{(\text{MAE}(k)/\text{MAE}(k+1))}{\log(N(k+1)/N(k))}. \end{aligned} \quad (38)$$

It is noted that the scheme is convergent against the selection of each fractional-order derivative and its convergence order increases as $\alpha \rightarrow 1$. Figures 2(c) and 2(b) contain the L_∞ -norm between consecutive solutions, i.e., $|U^{j+1} - U^j|_\infty$ and $|U_{i+1} - U_i|_\infty$ when $0 \leq i, j \leq N$, and $M = 500$. Again, it is found that the proposed scheme is very efficient, accurate, and reliable for this problem. It is also demonstrated that the solution is stable against the selection of fractional-order parameters and mesh parameters.

6. Results and Discussion

This section of our research work deals with a detailed overview of the key numerical findings and physical interpretations of different emerging parameters such as $Pr, M, \alpha, \beta, M^*$, and ϕ which are the Prandtl number, magnetic field parameter, fractional parameters, Joule's heating parameter, and volumetric fraction of nanoparticles, respectively. The behavior of the velocity profile $u(y, t)$ and temperature profile $\theta(y, t)$ and the effects of aforementioned physical parameters are deliberated, as well as graphical illustration is made via MAPLE. Discretization of time and spatial derivatives is done using finite difference methods. The coupled, nonlinear, and fractional model has been solved numerically by using finite difference method (FDM) which is a dominant tool to deal with such kind of problems.

Results are obtained by solving (17)-(18) with initial and boundary conditions illustrated in (20)-(21) and physical properties of nanoparticle in (17) and Table 1. Various suitable ranges of physical parameters ($0.01 \leq \lambda_1^\alpha \leq 0.5$), ($0 \leq Ha = M \leq 5$), ($1 \leq Gr \leq 5$), ($0.01 \leq \phi \leq 0.2$), and ($0.2 \leq \nu \leq 1$) for dimensionless velocity profile and ($0.01 \leq \lambda_1^\beta \leq 0.2$), ($0 \leq M^* \leq 2$), ($6.2 \leq Pr \leq 35$), ($0.01 \leq \phi \leq 0.2$), and ($0.2 \leq \nu \leq 1$) for heat transport are considered, and also particular exertion has been given on the effects of these parameters on the velocity and temperature profile.

Figure 3 depicts the impact of time relaxation parameter λ_1^α on momentum $u(y, t)$ of the fractional Maxwell fluids. With increase in fractional parameter α , momentum and thermal boundary layers decrease and even become their thinnest for $\alpha = 1$. Therefore, increasing relaxation parameters with range ($0.01 \leq \lambda_1^\alpha \leq 0.5$) has inverse impact on the velocity profile of the system, i.e., decrease occurs in the velocity profile.

Figure 4 shows the influence of magnetic field $Ha = M$ (the square of Hartmann Number) parameters on velocity profile $u(y, t)$. Both are inversely related, i.e., increasing value of Hartmann number Ha decreases the velocity profile. Since the increase in magnetic field parameter (Ha) gives hype to a well-known Lorentz force as this is the resistive force which

works against the flow direction, consequently it shows decrease in all the velocity components.

Figure 5 displays the behavior of Grashof number Gr on velocity profile $u(y, t)$ of fractional Maxwell fluids (FMFs) under the effects of magnetic field. Since Grashof number Gr is the ratio of buoyancy force to viscous force and is also known as buoyancy parameter, motion is resisted by the viscous force. So it was expected that an increase in Gr leads to an increase in the velocity profile of the bounded system, specifically near the wall of the bounded channel.

In Figure 6, results are drawn for volumetric fraction of nanoparticles against flow of fractional Maxwell fluids (FMFs). Addition of nanoparticles in base fluids increases their thickness (viscosity) which causes the internal resistance between the layers of flowing fluids, consequently decreasing the velocity $u(y, t)$ of the fluid. This is clearly deliberated in Figure 6.

Finally, the velocity profile against $\alpha = \beta = \nu$ (fractional parameters) is plotted in Figure 7, and results are verified as expected. The consequences of fractional order on fluid motion have an inverse relation. That is, for increasing values of fractional parameter α , the velocity profile decreases. However, $u(y, t)$ decreases for increasing values of α and attains its peak at $\alpha = 1$.

The heat transfer capability of the coupled and nonlinear model is illustrated in Figure 8. Here, the results for the temperature profile against time relaxation parameter λ_2^β are drawn and found as expected. Time relaxation is the key parameter used for characterization of the viscoelastic fluids, and it is the time in which a system relaxes under certain external conditions. Therefore, by the increase in λ_2^β , there results a decrease in the collision of particles within the fluids. This decreases the temperature profile $\theta(y, t)$ of fractional Maxwell nanofluids.

Figure 9 displays that magnetic field parameter impacts directly the temperature of the system because the enhancement in magnetic field parameter $Ha = M^*$ gives rise to a Lorentz force. This results in increase in the temperature profile $\theta(y, t)$ of the system.

Since Prandtl number Pr is the dimensionless number and is the ratio of momentum to thermal diffusivity. Since it is a fluid property, it does not have any dependence on flow type, as viscous forces exert a uniform effect on heat transfer for the whole of location of the channel. So, increase in Pr means heat transfer is favored to occur by momentum, not conduction. Therefore, increase in Pr decreases the temperature profile $\theta(y, t)$ of fractional Maxwell fluids (FMFs) as expressed in Figure 10.

Figure 11 gives the graphical results for influence of volume fraction of nanoparticles in base fluids on heat transfer capability of the system. Addition of nanoparticles in base fluids has a direct impact on enthalpy of the system. This results in entropy control of fluids during flow that is enhancement of thermal conductivity of fluids. The figure shows that increasing volume fraction ϕ enhances the thermal conductivity of the FMF with decrease in the temperature profile $\theta(y, t)$.

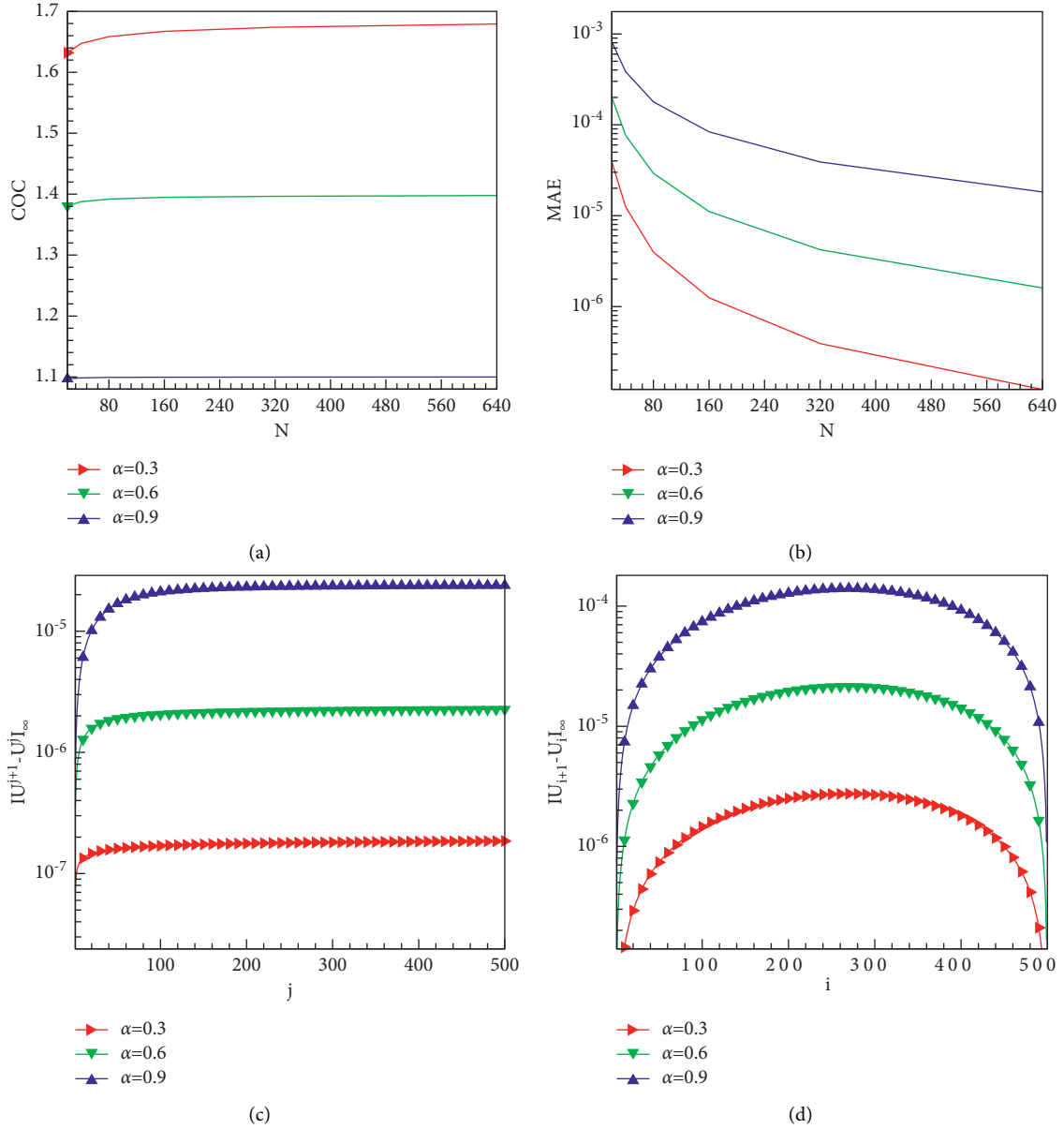


FIGURE 2: Code validation of the proposed scheme and varying time mesh sizes against (a) computational order of convergence (COC) and (b) maximum absolute error (MAE) and varying mesh sizes for (c) time and (d) space against L_∞ -norm between consecutive solutions.

Finally, Figure 12 depicts the effect of $(\alpha = \beta = \nu)$ on the temperature profile of the fractional Maxwell fluids. The fractional-order parameter and temperature profile are inversely proportional. It was expected and we obtained that increase in $(\alpha = \beta = \nu)$ decreases the heat transfer capability of the system.

The variations of skin friction coefficient and local Nusselt number are deliberated in Tables 2 and 3. It is noted

that the coefficient of skin friction increases with the increase in the physical parameters Gr , λ_1^α , and ϕ . The reverse behavior is observed against the variation of Hartmann number. Nusselt number impact against Pr , M^* , λ_2^β , and ϕ seems increasing. On the other hand, dominant impact of the fractional-order parameters $\alpha = \beta = \nu$ can be seen in Tables 2 and 3.

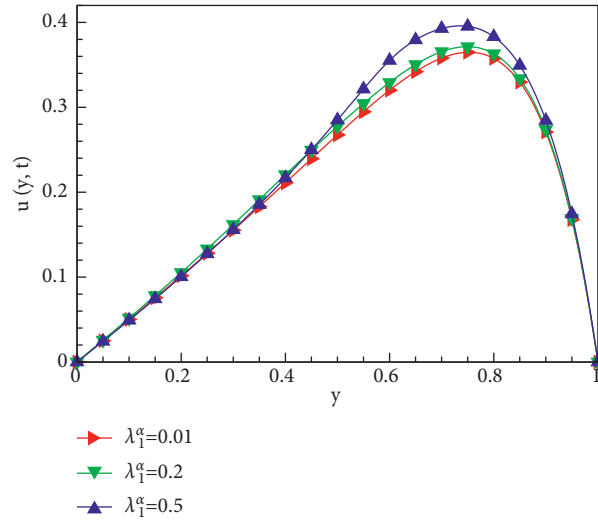


FIGURE 3: Influence of λ_1^α on u when $\alpha = \beta = 1$, $Gr = 5$, $Ha = 5$, $\lambda_2^\beta = 0.1$, $Pr = 6.2$, $M^* = 0.5$, and $\phi = 0.1$.

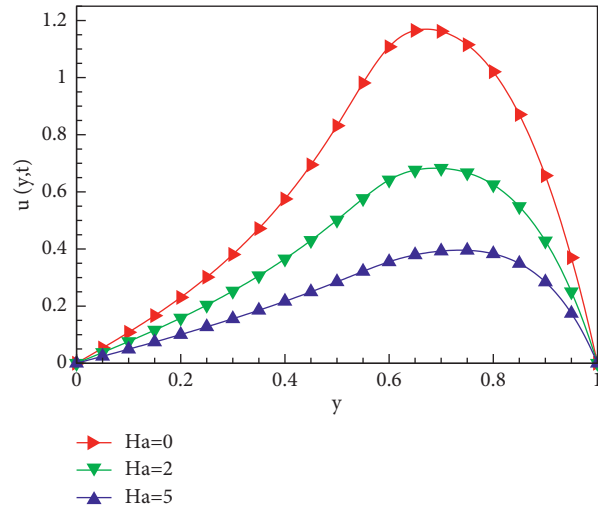


FIGURE 4: Influence of Ha on u when $\alpha = \beta = 1$, $\lambda_1^\alpha = 0.5$, $Gr = 5$, $\lambda_2^\beta = 0.1$, $Pr = 6.2$, $M^* = 0.5$, and $\phi = 0.1$.

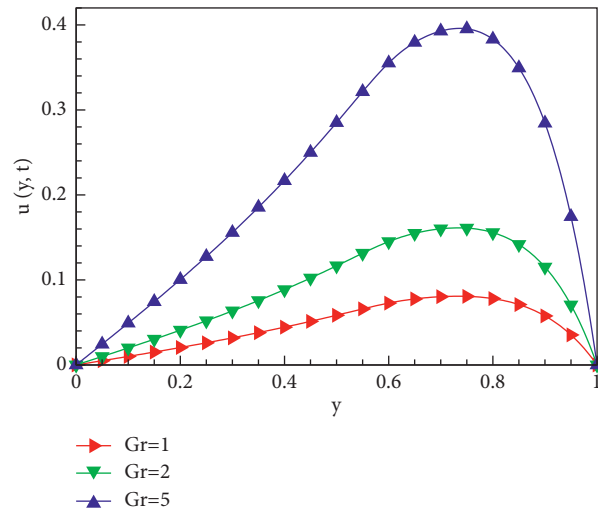


FIGURE 5: Influence of Gr on u when $\alpha = \beta = 1$, $\lambda_1^\alpha = 0.5$, $Ha = 5$, $\lambda_2^\beta = 0.1$, $Pr = 6.2$, $M^* = 0.5$, and $\phi = 0.1$.

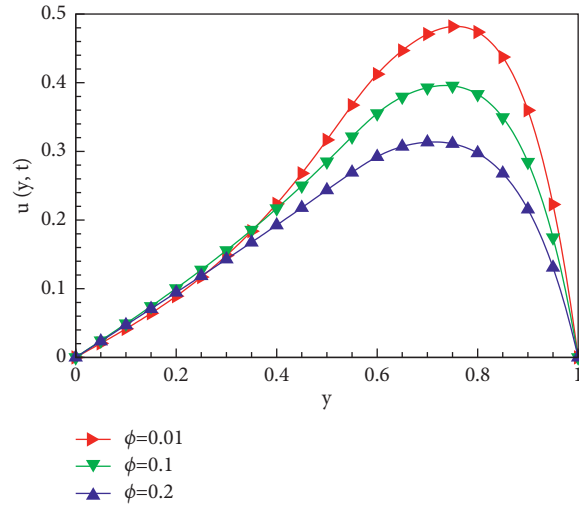


FIGURE 6: Influence of ϕ on u when $\alpha = \beta = 1$, $\lambda_1^\alpha = 0.5$, $Gr = 5$, $Ha = 5$, $\lambda_2^\beta = 0.1$, $Pr = 6.2$, and $M^* = 0.5$.

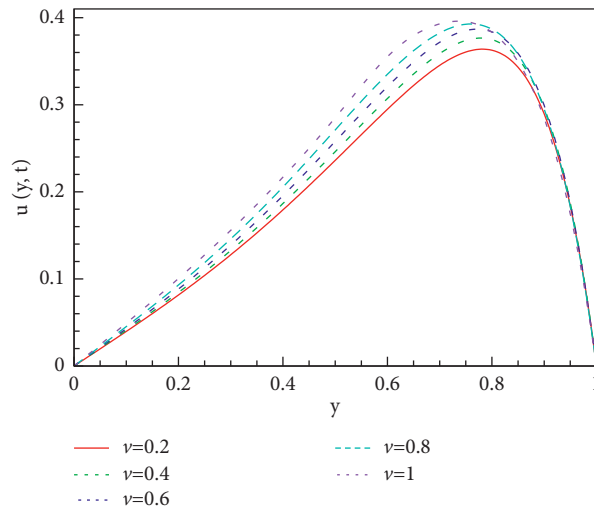


FIGURE 7: Influence of $\alpha = \beta = \gamma$ on u when $\lambda_1^\alpha = 0.5$, $Gr = 5$, $Ha = 5$, $\lambda_2^\beta = 0.1$, $Pr = 6.2$, $M^* = 0.5$, and $\phi = 0.1$.

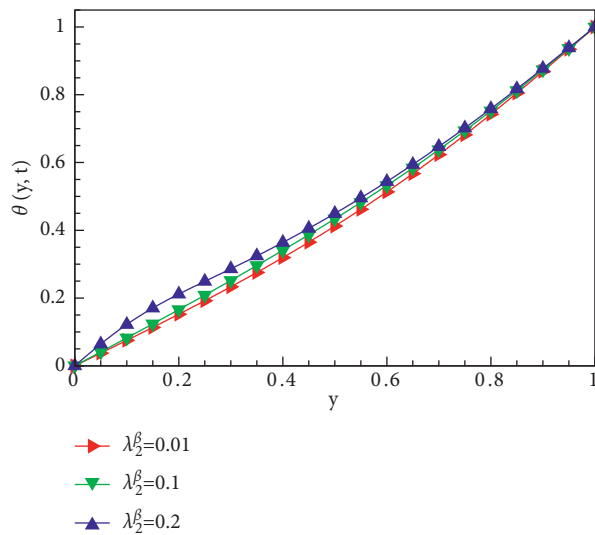


FIGURE 8: Influence of λ_2^β on θ when $\alpha = \beta = 1$, $\lambda_1^\alpha = 0.5$, $Gr = 5$, $Ha = 5$, $Pr = 6.2$, $M^* = 0.5$, and $\phi = 0.1$.

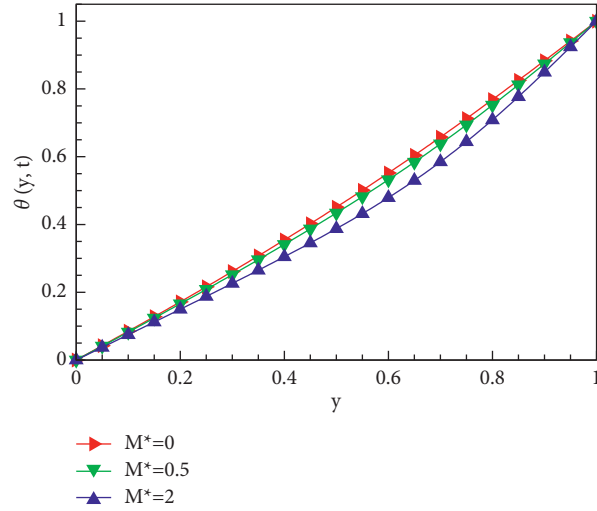


FIGURE 9: Influence of M^* on θ when $\alpha = \beta = 1$, $\lambda_1^\alpha = 0.5$, $Gr = 5$, $Ha = 5$, $\lambda_2^\beta = 0.1$, $Pr = 6.2$, and $\phi = 0.1$.

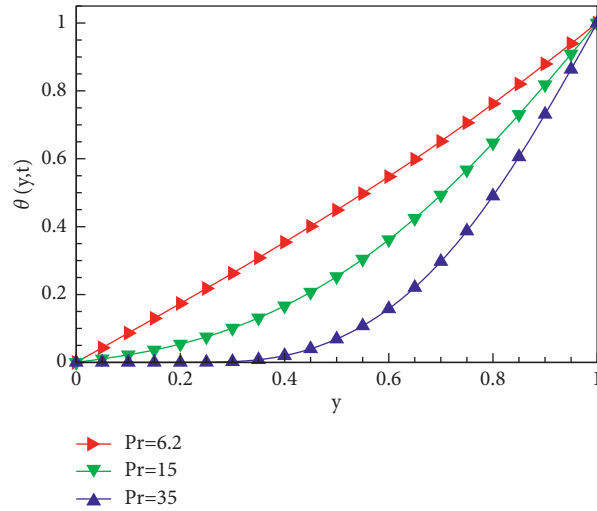


FIGURE 10: Influence of Pr on θ when $\alpha = \beta = 1$, $\lambda_1^\alpha = 0.5$, $Gr = 5$, $Ha = 5$, $\lambda_2^\beta = 0.1$, $M^* = 0.5$, and $\phi = 0.1$.

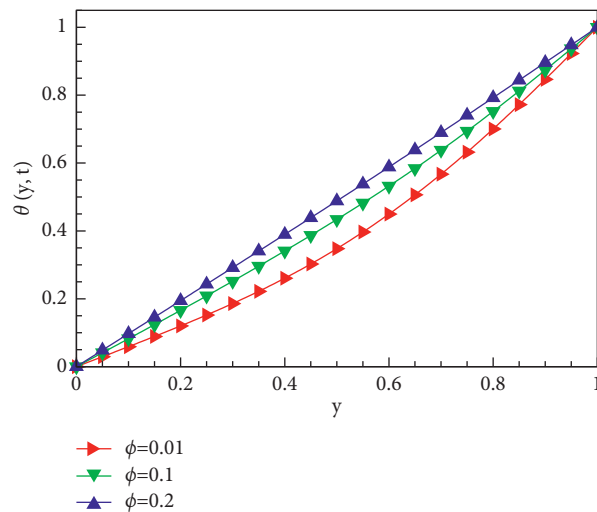


FIGURE 11: Influence of ϕ on θ when $\alpha = \beta = 1$, $\lambda_1^\alpha = 0.5$, $Gr = 5$, $Ha = 5$, $\lambda_2^\beta = 0.1$, $Pr = 6.2$, and $M^* = 0.5$.

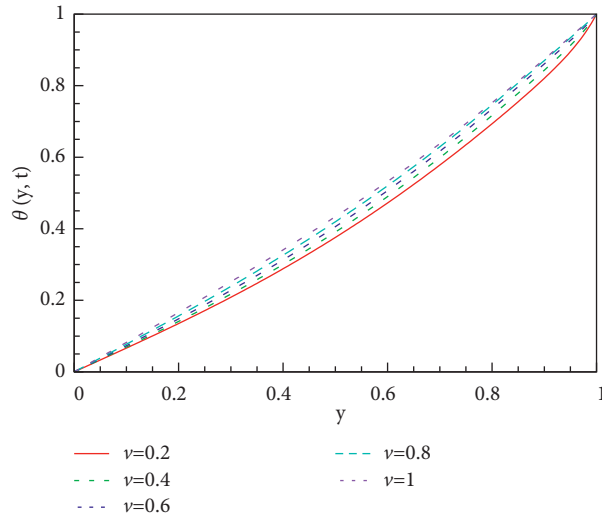


FIGURE 12: Influence of $\alpha = \beta = \nu$ on θ when $\lambda_1^\alpha = 0.5$, $Gr = 5$, $Ha = 5$, $\lambda_2^\beta = 0.1$, $Pr = 6.2$, $M^* = 0.5$, and $\phi = 0.1$.

TABLE 2: Skin friction analysis against different physical parameters when $\lambda_2^\beta = 0.1$, $Pr = 6.8$, $M^* = 0.5$, and $Re = 10$.

Gr	M	λ_1^α	ϕ	$\nu = 0.4$	$\nu = 0.7$	$\nu = 1$	
0.1	10	0.5	0.1	0.0047	0.0051	0.0058	
2				0.0934	0.1016	0.1160	
5				0.2316	0.2519	0.2877	
	0			1.0966	0.6819	0.4058	
	2			1.0730	0.7047	0.4348	
	5			1.0600	0.7500	0.4882	
				0.1	0.4177	0.4119	0.4058
				0.3	0.4513	0.4445	0.4348
				0.5	0.5166	0.5044	0.4882
					0.01	0.3642	0.4105
			0.15	0.3753	0.4429	0.4049	
			0.25	0.4063	0.4910	0.4304	

TABLE 3: Nusselt number analysis against different physical parameters when $\lambda_1^\alpha = 0.5$, $M = 10$, $Gr = 5$, and $Re = 10$.

Pr	M^*	λ_2^β	ϕ	$\nu = 0.4$	$\nu = 0.7$	$\nu = 1$		
3.94	0.5	0.1	0.1	0.9142	0.7511	0.2134		
6.2				0.9710	0.8129	0.2105		
15				0.9999	0.8817	0.2038		
3.94	0.1	0.5		0.7087	0.6799	0.6384		
	2			0.7687	0.7363	0.6894		
	5			0.8458	0.8070	0.7505		
	0.5			0.01	0.7543	0.7024	0.6552	
				0.1	0.7601	0.7617	0.7558	
				0.2	0.7672	0.8374	1.3188	
					0.01	0.4582	0.7967	0.9335
					0.15	0.4928	0.8582	0.9823
					0.25	0.5854	0.9140	0.9957

7. Conclusion

An unsteady flow and heat transfer for the coupled and nonlinear model of fractional Maxwell fluids is solved by using power law kernel. Findings are done under the effects of magnetic fields within a channel. Codes are developed and executed to obtain the numerical results by applying the finite difference method for discretization of spatial and time derivatives. Some key finding are illustrated as follows:

- (a) Fractional-order parameters α and β have a direct impact on velocity profile and inverse impact on temperature profile.
- (b) The velocity and temperature are enhanced for a high value of the unsteadiness parameter. Velocity is slightly decreasing for higher values of Reynolds number Re , while a smaller value of Reynolds number has more prominent impact on velocity and temperature.
- (c) Addition of the nanoparticles to base fluids enhances the thermal conductivity by increasing the surface. Consequently, volumetric concentration of nanoparticles ϕ in base fluids results in decrease in the temperature profile of the FMF.
- (d) Finally, the chosen numerical technique of the finite difference method shows stable results and gives new direction to such investigation.
- (e) This method can be extended for more numerous types of physical sciences with complex geometries.

This simplified research problem can be generalized to express the effects of viscosity (viscous dissipation), variable thermal conductivity, and multidimensional MHD flow regime and temperature profile of non-Newtonian nanofluids. Many opportunities for further investigation exist in this direction for detailed study.

Abbreviations

u (m/s):	Velocity
θ (K):	Temperature
ρ_{nf} (kg/m ³):	Density
μ_{nf} (kg/ms):	Dynamic viscosity
k_{nf} (W/mK):	Thermal conductivity of nanofluid
β_{θ} (K ⁻¹):	Volumetric thermal expansion coefficient
g (m/s ²):	Gravitational acceleration
$(C_p)_{nf}$:	Heat capacity of nanoparticles
σ_{nf} (S/m):	Electrical conductivity of nanoparticles
ν_{nf} (m ² /s):	Kinematic viscosity of nanoparticles
ϕ :	Volume fraction of nanoparticles.

Data Availability

No data were used to support this study.

Conflicts of Interest

The authors declare that they have no conflicts of interest.

Acknowledgments

This research was funded by the Princess Nourah bint Abdulrahman University Researchers Supporting Project number (PNURSP2022R152), Princess Nourah bint Abdulrahman University, Riyadh, Saudi Arabia. Also, the authors extend their appreciation to the Deanship of Scientific Research at King Khalid University, Abha, Saudi Arabia for funding this work through research groups program under grant number R.G.P-2/135/42.

References

- [1] M. Saqib, F. Ali, I. Khan, N. A. Sheikh, S. A. A. Jan, and U. H. Sami, "Exact solutions for free convection flow of generalized Jeffrey fluid: a Caputo-Fabrizio fractional model," *Alexandria Engineering Journal*, vol. 57, no. 3, pp. 1849–1858, 2018.
- [2] M. Saqib, S. Shafie, I. Khan, Y.-M. Chu, and K. S. Nisar, "Symmetric MHD channel flow of nonlocal fractional model of BTF containing hybrid nanoparticles," *Symmetry*, vol. 12, no. 4, p. 663, 2020.
- [3] M. Saqib, A. R. K. Mohd, N. F. Mohammad, D. L. C. Chuan, and S. Shafie, "Application of fractional derivative without singular and local kernel to enhanced heat transfer in CNTs nanofluid over an inclined plate," *Symmetry*, vol. 12, no. 5, p. 768, 2020.
- [4] F. Ali, M. Saqib, I. Khan, and N. A. Sheikh, "Application of Caputo-Fabrizio derivatives to MHD free convection flow of generalized Walters'-B fluid model," *The European Physical Journal Plus*, vol. 131, no. 10, pp. 1–10, 2016.
- [5] N. A. Sheikh, F. Ali, M. Saqib et al., "Comparison and analysis of the Atangana-Baleanu and Caputo-Fabrizio fractional derivatives for generalized Casson fluid model with heat generation and chemical reaction," *Results in Physics*, vol. 7, pp. 789–800, 2017.
- [6] M. I. Asjad, M. D. Ikram, and R. Ali, "New analytical solutions of heat transfer flow of clay-water base nanoparticles with the application of novel hybrid fractional derivative," *Thermal Science*, vol. 24, no. Suppl. 1, pp. 343–350, 2020.
- [7] Y.-M. Chu, M. D. Ikram, M. I. Asjad, A. Ahmadian, and F. Ghaemi, "Influence of hybrid nanofluids and heat generation on coupled heat and mass transfer flow of a viscous fluid with novel fractional derivative," *Journal of Thermal Analysis and Calorimetry*, vol. 144, no. 6, pp. 2057–2077, 2021.
- [8] T. Hayat, A. Inayatullah, A. Alsaedi, and B. Ahmad, "Thermo diffusion and diffusion thermo impacts on bioconvection Walter-B nanomaterial involving gyrotactic microorganisms," *Alexandria Engineering Journal*, vol. 60, no. 6, pp. 5537–5545, 2021.
- [9] A. Tassaddiq, I. Khan, K. Sooppy Nisar, and J. Singh, "MHD flow of a generalized Casson fluid with Newtonian heating: a fractional model with Mittag-Leffler memory," *Alexandria Engineering Journal*, vol. 59, no. 5, pp. 3049–3059, 2020.
- [10] J. C. Maxwell, "On the dynamical theory of gases," *Proceedings of the Royal Society of London*, vol. 15, pp. 167–171, 1866.
- [11] M. Takashima, "The effect of a magnetic field on thermal instability in a layer of Maxwell fluid," *Physics Letters A*, vol. 33, no. 6, pp. 371–372, 1970.
- [12] J. Choi, Z. Rusak, and J. Tichy, "Maxwell fluid suction flow in a channel," *Journal of Non-newtonian Fluid Mechanics*, vol. 85, no. 2-3, pp. 165–187, 1999.

- [13] C. Fetecau and C. Fetecau, "A new exact solution for the flow of a Maxwell fluid past an infinite plate," *International Journal of Non-linear Mechanics*, vol. 38, no. 3, pp. 423–427, 2003.
- [14] C. Fetecau and C. Fetecau, "The Rayleigh-Stokes-Problem for a fluid of Maxwellian type," *International Journal of Non-linear Mechanics*, vol. 38, no. 4, pp. 603–607, 2003.
- [15] C. Friedrich, "Relaxation and retardation functions of the Maxwell model with fractional derivatives," *Rheologica Acta*, vol. 30, no. 2, pp. 151–158, 1991.
- [16] P. M. Jordan, A. Puri, and G. Boros, "On a new exact solution to Stokes' first problem for Maxwell fluids," *International Journal of Non-linear Mechanics*, vol. 39, no. 8, pp. 1371–1377, 2004.
- [17] F. Olsson and J. Yström, "Some properties of the upper convected Maxwell model for viscoelastic fluid flow," *Journal of Non-newtonian Fluid Mechanics*, vol. 48, no. 1-2, pp. 125–145, 1993.
- [18] L. Liu and F. Liu, "Boundary layer flow of fractional Maxwell fluid over a stretching sheet with variable thickness," *Applied Mathematics Letters*, vol. 79, pp. 92–99, 2018.
- [19] M. Zhang, M. Shen, F. Liu, and H. Zhang, "A new time and spatial fractional heat conduction model for Maxwell nanofluid in porous medium," *Computers & Mathematics with Applications*, vol. 78, no. 5, pp. 1621–1636, 2019.
- [20] N. Sadiq, M. Imran, C. Fetecau, and N. Ahmed, "Rotational motion of fractional Maxwell fluids in a circular duct due to a time-dependent couple," *Boundary Value Problems*, vol. 2019, no. 1, pp. 1–11, 2019.
- [21] Y. Bai, L. Huo, Y. Zhang, and Y. Jiang, "Flow, heat and mass transfer of three-dimensional fractional Maxwell fluid over a bidirectional stretching plate with fractional Fourier's law and fractional Fick's law," *Computers & Mathematics with Applications*, vol. 78, no. 8, pp. 2831–2846, 2019.
- [22] X. Chen, W. Yang, X. Zhang, and F. Liu, "Unsteady boundary layer flow of viscoelastic MHD fluid with a double fractional Maxwell model," *Applied Mathematics Letters*, vol. 95, pp. 143–149, 2019.
- [23] N. Raza and M. A. Ullah, "A comparative study of heat transfer analysis of fractional Maxwell fluid by using Caputo and Caputo-Fabrizio derivatives," *Canadian Journal of Physics*, vol. 98, no. 1, pp. 89–101, 2020.
- [24] S. U. Choi and J. A. Eastman, *Enhancing thermal Conductivity of Fluids with Nanoparticles*, Argonne National Lab., IL, USA, 1995.
- [25] R. K. Tiwari and M. K. Das, "Heat transfer augmentation in a two-sided lid-driven differentially heated square cavity utilizing nanofluids," *International Journal of Heat and Mass Transfer*, vol. 50, no. 9-10, pp. 2002–2018, 2007.
- [26] M. Saqib, I. Khan, and S. Shafie, "Application of Atangana-Baleanu fractional derivative to MHD channel flow of CMC-based-CNT's nanofluid through a porous medium," *Chaos, Solitons & Fractals*, vol. 116, pp. 79–85, 2018.
- [27] M. Shamshuddin and M. R. Eid, "Magnetized nanofluid flow of ferromagnetic nanoparticles from parallel stretchable rotating disk with variable viscosity and thermal conductivity," *Chinese Journal of Physics*, vol. 74, pp. 20–37, 2021.
- [28] M. Aleem, M. Imran Asjad, M. S. R. Chowdhury, and A. Hussanan, "Analysis of mathematical model of fractional viscous fluid through a vertical rectangular channel," *Chinese Journal of Physics*, vol. 61, pp. 336–350, 2019.
- [29] W. Jamshed, C. Şirin, F. Selimefendigil, M. Shamshuddin, Y. Altowairqi, and M. R. Eid, "Thermal characterization of coolant maxwell type nanofluid flowing in parabolic trough solar collector (PTSC) used inside solar powered ship application," *Coatings*, vol. 11, no. 12, p. 1552, 2021.
- [30] M. Shamshuddin, S. R. Mishra, O. A. Bég, T. A. Bég, and K. Ali, "Computation of radiative Marangoni (thermocapillary) magnetohydrodynamic convection in a Cu-water based nanofluid flow from a disk in porous media: smart coating simulation," *Heat Transfer*, vol. 50, no. 3, pp. 1931–1950, 2021.
- [31] T. Hayat, T. Muhammad, S. A. Shehzad, G. Q. Chen, and I. A. Abbas, "Interaction of magnetic field in flow of Maxwell nanofluid with convective effect," *Journal of Magnetism and Magnetic Materials*, vol. 389, pp. 48–55, 2015.
- [32] A. Jafarimoghaddam, "On the homotopy analysis method (HAM) and homotopy perturbation method (HPM) for a nonlinearly stretching sheet flow of Eyring-Powell fluids," *Engineering Science and Technology, an International Journal*, vol. 22, no. 2, pp. 439–451, 2019.
- [33] C. Sravanthi and R. Gorla, "Effects of heat source/sink and chemical reaction on MHD Maxwell nanofluid flow over a convectively heated exponentially stretching sheet using homotopy analysis method," *International Journal of Applied Mechanics and Engineering*, vol. 23, no. 1, 2018.
- [34] T. Anwar, P. Kumam, I. Khan, and W. Watthayu, "Heat transfer enhancement in unsteady MHD natural convective flow of CNTs Oldroyd-B nanofluid under ramped wall velocity and ramped wall temperature," *Entropy*, vol. 22, no. 4, p. 401, 2020.
- [35] A. Q. Khan and A. Rasheed, "Numerical simulation of fractional Maxwell fluid flow through forchheimer medium," *International Communications in Heat and Mass Transfer*, vol. 119, Article ID 104872, 2020.
- [36] N. A. Sheikh, F. Ali, I. Khan, M. Gohar, and M. Saqib, "On the applications of nanofluids to enhance the performance of solar collectors: a comparative analysis of Atangana-Baleanu and Caputo-Fabrizio fractional models," *The European Physical Journal Plus*, vol. 132, no. 12, pp. 1–11, 2017.
- [37] C.-C. Wang, "Mathematical principles of mechanics and electromagnetism: Part A: Analytical and continuum mechanics," *Springer Science & Business Media*, vol. 16, 2013.
- [38] M. Saqib, I. Khan, and S. Shafie, "Application of fractional differential equations to heat transfer in hybrid nanofluid: modeling and solution via integral transforms," *Advances in Difference Equations*, vol. 2019, no. 1, pp. 1–18, 2019.
- [39] J. Zhao, L. Zheng, X. Zhang, and F. Liu, "Convection heat and mass transfer of fractional MHD Maxwell fluid in a porous medium with Soret and Dufour effects," *International Journal of Heat and Mass Transfer*, vol. 103, pp. 203–210, 2016.
- [40] C. Cattaneo, "A form of heat-conduction equations which eliminates the paradox of instantaneous propagation," *Comptes Rendus*, vol. 247, p. 431, 1958.
- [41] L. Liu, L. Zheng, and F. Liu, "Time fractional Cattaneo-Christov anomalous diffusion in comb frame with finite length of fingers," *Journal of Molecular Liquids*, vol. 233, pp. 326–333, 2017.
- [42] T. A. Yusuf, F. Mabood, W. A. Khan, and J. A. Gbadeyan, "Irreversibility analysis of Cu-TiO₂-H₂O hybrid-nanofluid impinging on a 3-D stretching sheet in a porous medium with nonlinear radiation: Darcy-Forchheimer's model," *Alexandria Engineering Journal*, vol. 59, no. 6, pp. 5247–5261, 2020.
- [43] S. Hazarika, S. Ahmed, and A. J. Chamkha, "Investigation of nanoparticles Cu, Ag and Fe₃O₄ on thermophoresis and viscous dissipation of MHD nanofluid over a stretching sheet in a porous regime: a numerical modeling," *Mathematics and Computers in Simulation*, vol. 182, pp. 819–837, 2021.

- [44] J. Zhao, L. Zheng, X. Zhang, and F. Liu, "Unsteady natural convection boundary layer heat transfer of fractional Maxwell viscoelastic fluid over a vertical plate," *International Journal of Heat and Mass Transfer*, vol. 97, pp. 760–766, 2016.
- [45] A. Q. Khan and A. Rasheed, "Mixed convection magneto-hydrodynamics flow of a nanofluid with heat transfer: a numerical study," *Mathematical Problems in Engineering*, vol. 2019, Article ID 8129564, 14 pages, 2019.